
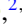



Enhanced magnetoelectric effect near a field-driven zero-temperature quantum phase transition of the spin-1/2 Heisenberg-Ising ladder

Jozef Strečka ¹, Lucia Gálisová ^{2,*}, and Taras Verkholyak ³

¹*Institute of Physics, Faculty of Science, P. J. Šafárik University, Park Angelinum 9, 040 01 Košice, Slovak Republic*

²*Institute of Manufacturing Management, Faculty of Manufacturing Technologies with the seat in Prešov, Technical University of Košice, Bayerova 1, 080 01 Prešov, Slovak Republic*

³*Institute for Condensed Matter Physics, National Academy of Sciences of Ukraine, Svientsitskii Street 1, 790 11 L'viv, Ukraine*



(Received 20 October 2019; published 3 January 2020)

The magnetoelectric effect of a spin-1/2 Heisenberg-Ising ladder in the presence of external electric and magnetic fields is rigorously examined by taking into account the Katsura-Nagaosa-Balatsky mechanism. It is shown that an applied electric field may control the quantum phase transition between a Néel (stripy) ordered phase and a disordered paramagnetic phase. The staggered magnetization vanishes according to a power law with an Ising-type critical exponent 1/8, the electric polarization exhibits a weak singularity, and the dielectric susceptibility shows a logarithmic divergence at this particular quantum phase transition. The external electric field may alternatively invoke a discontinuous phase transition accompanied with abrupt jumps of the dielectric polarization and susceptibility on the assumption that the external magnetic field becomes nonzero.

DOI: [10.1103/PhysRevE.101.012103](https://doi.org/10.1103/PhysRevE.101.012103)

I. INTRODUCTION

Although early investigations of the magnetoelectric effect (MEE) date back to the 19th century [1], this phenomenon is the subject of renewed research interest mainly due to its wide application potential in modern technologies [2]. A dependence of the magnetization on an electric field and the electric polarization on a magnetic field can be described by several alternative mechanisms. According to the Katsura-Nagaosa-Balatsky (KNB) mechanism [3] the dielectric polarization $\mathbf{p}_{i,j}$ is connected to the spin current $\mathbf{j}_{i,j}$ between a pair of neighboring spins \mathbf{s}_i and \mathbf{s}_j through the expression

$$\mathbf{p}_{i,j} \propto \mathbf{e}_{i,j} \times \mathbf{j}_{i,j}, \quad (1)$$

where $\mathbf{e}_{i,j}$ is the unit vector pointing from the i th to j th lattice site and the spin current $\mathbf{j}_{i,j} \propto \mathbf{s}_i \times \mathbf{s}_j$ is proportional to the antisymmetric Dzyaloshinskii-Moriya (DM) term [4,5] on the assumption that two neighboring spins are coupled through an isotropic exchange interaction.

An experimental observation of the striking magnetoelectric response of certain quasi-one-dimensional magnetic materials is another reason for the current substantial effort aimed at a more comprehensive understanding of the MEE conditioned by the KNB mechanism [6,7]. Up to now, rigorous studies of the MEE arising from the KNB mechanism have been limited to a few paradigmatic quantum spin chains such as the XXZ Heisenberg chain [8], the XY chain with a three-spin interaction [9,10], the XY zigzag chain [11], and the quantum compass chain [12].

The main goal of the present paper is to extend the aforementioned class of one-dimensional quantum spin models.

For this purpose, we will examine the spin-1/2 Heisenberg-Ising ladder simultaneously in a longitudinal magnetic field and an electric field applied along the y axis in space. As we demonstrate hereafter, the proposed quantum spin model represents a very good tool for the rigorous study of an enhanced MEE conditioned by the KNB mechanism near a continuous quantum phase transition in the ground state.

The outline of the paper is as follows. In Sec. II we define the quantum model and briefly mention the basic steps leading to a rigorous solution of its ground state. The most interesting numerical results dealing with the MEE will be presented in Secs. III and IV. Finally, some summarized ideas are posted in Sec. V.

II. MODEL AND ITS SOLUTION

Let us consider the quantum spin-1/2 Heisenberg-Ising ladder defined through the Hamiltonian (see Fig. 1)

$$\mathcal{H} = \sum_{i=1}^N [J_H \mathbf{s}_{1,i} \cdot \mathbf{s}_{2,i} + J_l (s_{1,i}^z s_{1,i+1}^z + s_{2,i}^z s_{2,i+1}^z) - h (s_{1,i}^z + s_{2,i}^z) - E (s_{1,i}^y s_{2,i}^x - s_{1,i}^x s_{2,i}^y)], \quad (2)$$

where $\mathbf{s}_{l,i} \equiv (s_{l,i}^x, s_{l,i}^y, s_{l,i}^z)$ represents the standard spin-1/2 operator for the i th site of the l th leg ($i = 1, 2, \dots, N$; $l = 1, 2$), the parameter $J_H > 0$ denotes the antiferromagnetic Heisenberg intrarung interaction, $J_l > 0$ ($J_l < 0$) labels the antiferromagnetic (ferromagnetic) Ising intraleg interaction, and N denotes the total number of the ladder's rungs under the periodic boundary condition $\mathbf{s}_{l,N+1} \equiv \mathbf{s}_{l,1}$. Finally, the last two terms in Eq. (2) represent the standard Zeeman term associated with the magnetic field h applied along the z axis and the inverse DM term connected to the electric field E applied

*galisova.lucia@gmail.com

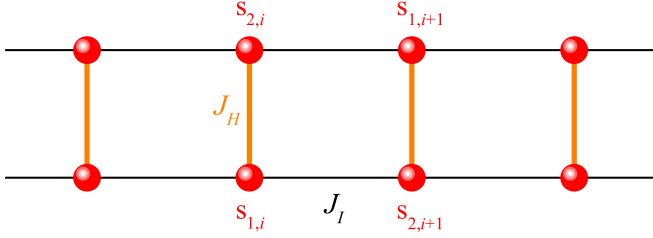


FIG. 1. A part of the quantum spin-1/2 Heisenberg-Ising two-leg ladder. Thick orange (thin black) lines represent the Heisenberg intrarung (the Ising intraleg) interactions in the system.

along the y axis, which affects the corresponding component of the dielectric polarization (1), respectively. By supposing that the ladder's rungs are aligned along the x axis in space, i.e., $\mathbf{e}_{(1,i),(2,i)} = (1, 0, 0)$ in Eq. (1), the dielectric polarization $p_i^y = s_{1,i}^y s_{2,i}^y - s_{1,i}^x s_{2,i}^x$ is prescribed to the i th rung. Note that the dielectric dipole moment is imposed to be generated on the Heisenberg rungs only, whereas the Ising bonds along the legs do not exhibit any magnetoelectric connection.

The DM term associated with the electric field can be eliminated from the Hamiltonian (2) by performing a local spin-rotation transformation around the z axis by the specific angle $\varphi = \tan^{-1}(E/J_H)$ [13]. As a result, one gets the Hamiltonian of the spin-1/2 Heisenberg-Ising ladder with the effective XXZ intrarung interaction and the Ising intraleg interaction in a magnetic field,

$$\mathcal{H} = \sum_{i=1}^N \left[\sqrt{J_H^2 + E^2} (s_{1,i}^x s_{2,i}^x + s_{1,i}^y s_{2,i}^y) + J_H s_{1,i}^z s_{2,i}^z + J_I (s_{1,i}^z s_{1,i+1}^z + s_{2,i}^z s_{2,i+1}^z) - h (s_{1,i}^z + s_{2,i}^z) \right], \quad (3)$$

which can be alternatively viewed as a special case of the frustrated spin-1/2 Heisenberg-Ising ladders exactly solved in recent works [14–16]. Therefore, it is sufficient to closely follow the approach elaborated in Ref. [14] to get a rigorous solution for the ground state of the investigated quantum spin model. First, we define the eigenstates of the XXZ bonds on the rungs,

$$\begin{aligned} |\phi_{0,\pm}^i\rangle &= \frac{1}{\sqrt{2}} (|\downarrow_{1,i} \uparrow_{2,i}\rangle \pm |\uparrow_{1,i} \downarrow_{2,i}\rangle), \\ |\phi_{1,\pm}^i\rangle &= \frac{1}{\sqrt{2}} (|\uparrow_{1,i} \uparrow_{2,i}\rangle \pm |\downarrow_{1,i} \downarrow_{2,i}\rangle), \end{aligned} \quad (4)$$

where the states $|\phi_{0,\pm}^i\rangle$ ($|\phi_{1,\pm}^i\rangle$) belong to the subspace with $(S_i^z)^2 = (s_{1,i}^z + s_{2,i}^z)^2 = 0$ (1). In the next step we introduce the pseudospin notations for the bond states as $|\phi_{0,-}^i\rangle = |\downarrow\rangle_0^i$, $|\phi_{0,+}^i\rangle = |\uparrow\rangle_0^i$ [for $(S_i^z)^2 = 0$ subspace], and $|\phi_{1,-}^i\rangle = |\downarrow\rangle_1^i$, $|\phi_{1,+}^i\rangle = |\uparrow\rangle_1^i$ [for $(S_i^z)^2 = 1$ subspace]. We also need to set new spin operators \tilde{s}_i^α ($\alpha = x, y, z$) acting on the pseudospin basis as well as the binary variable $n_i = 0$ and 1 assigned to $(S_i^z)^2 = 0$ and 1 states of the i th rung (dimer), respectively. By straightforward calculation one can establish the following

relations for the spin operators,

$$\begin{aligned} s_{1,i}^z &= (2n_i - 1)\tilde{s}_i^z, & s_{2,i}^z &= \tilde{s}_i^z, \\ s_{1,i}^x s_{2,i}^x &= \tilde{s}_i^x, & s_{1,i}^y s_{2,i}^y &= (1 - 2n_i)\frac{\tilde{s}_i^y}{2}, & s_{1,i}^z s_{2,i}^z &= \frac{1}{4}(2n_i - 1). \end{aligned}$$

Consequently, it results in the following equivalent pseudospin representation of the Hamiltonian (3),

$$\mathcal{H} = \sum_{i=1}^N \left\{ 2J_I [n_i n_{i+1} + (1 - n_i)(1 - n_{i+1})] \tilde{s}_i^x \tilde{s}_{i+1}^x + \sqrt{J_H^2 + E^2} (1 - n_i) \tilde{s}_i^z - 2h n_i \tilde{s}_i^x + \frac{J_H}{4} (2n_i - 1) \right\}. \quad (5)$$

It has been verified in Ref. [14] that the lowest-energy eigenstates derived from the effective Hamiltonian (5) of the spin-1/2 Heisenberg-Ising ladder in zero magnetic field ($h = 0$) follow from two exactly solved spin-chain models, namely, the spin-1/2 Ising chain in a transverse magnetic field [17] acquired from the effective Hamiltonian (5) by assuming all rung states in the $(S_i^z)^2 = 0$ subspace ($n_i = 0$) and the spin-1/2 Ising chain in a longitudinal magnetic field [18] acquired from the effective Hamiltonian (5) by considering all rung states in the $(S_i^z)^2 = 1$ subspace ($n_i = 1$). In a nonzero magnetic field ($h \neq 0$) one additionally has to consider another exactly solvable effective spin-chain model acquired from the effective Hamiltonian (5) by assuming a regular alternation of the singlet and triplet states on odd and even rungs that correspond to $n_{2i-1} = 0$ and $n_{2i} = 1$ or vice versa [14]. From this point of view, the exact solution for a ground state of the spin-1/2 Heisenberg-Ising ladder in electric and magnetic fields defined through the Hamiltonian (2) is formally completed.

III. MEE IN ZERO MAGNETIC FIELD

The ground-state energy of the spin-1/2 Heisenberg-Ising ladder in zero magnetic field ($h = 0$) follows from the formula

$$\mathcal{E}_{\text{GS}} \equiv \frac{1}{N} \langle \mathcal{H} \rangle = -\frac{J_H}{4} - \frac{\sqrt{J_H^2 + E^2} + |J_I|}{\pi} \mathbf{E}(a), \quad (6)$$

where $\mathbf{E}(a) = \int_0^{\frac{\pi}{2}} d\phi \sqrt{1 - a^2 \sin^2 \phi}$ is the complete elliptic integral of the second kind with $a^2 = \frac{4|\lambda|}{(1+|\lambda|)^2}$ and $\lambda = \frac{J_I}{\sqrt{J_H^2 + E^2}}$. The ground-state energy (6) has a singularity at $|\lambda| = 1$ ($|E_c| = \sqrt{J_I^2 - J_H^2}$), which relates to a quantum phase transition between the quantum paramagnetic (QPM) phase emergent for $|\lambda| \leq 1$ and either a Néel or stripe-leg (SL) phase emergent for $|\lambda| > 1$ depending on whether $J_I > 0$ or $J_I < 0$, respectively. While the Néel and stripy spin orders are quite analogous and can be characterized through the nonzero staggered magnetization, this order parameter becomes zero within the disordered QPM phase,

$$m_s^z \equiv \frac{1}{2} \langle |s_{1,i}^z - s_{2,i}^z| \rangle = \begin{cases} \frac{1}{2} \left(1 - \frac{1}{\lambda^2}\right)^{1/8} & \text{if } |\lambda| > 1, \\ 0 & \text{if } |\lambda| \leq 1. \end{cases} \quad (7)$$

Obviously, the staggered magnetization m_s^z displays a steep power-law decline with the Ising-type critical exponent

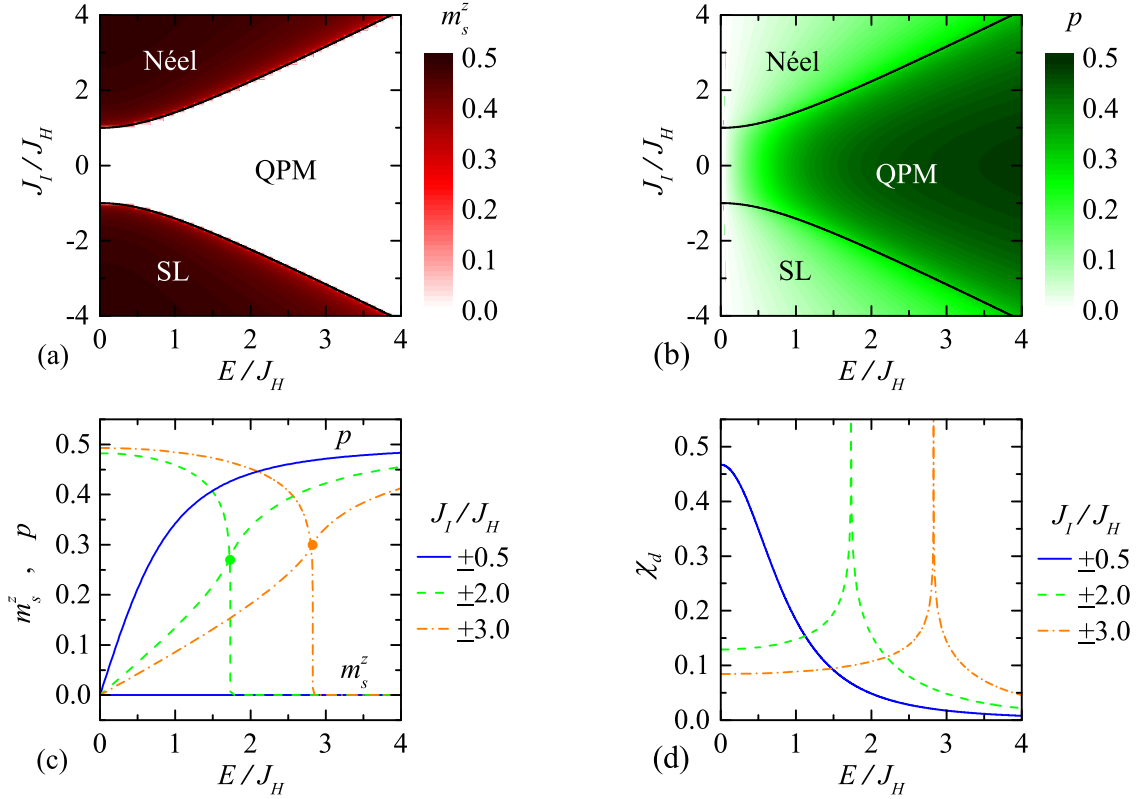


FIG. 2. The density plot of (a) the staggered magnetization m_s^z and (b) the dielectric polarization p as ground-state phase diagrams in the E/J_H - J_I/J_H plane, together with the electric field variations of (c) the staggered magnetization m_s^z and the dielectric polarization p , and (d) the dielectric susceptibility χ_d for the interaction ratios $J_I/J_H = \pm 0.5, \pm 2.0, \pm 3.0$.

$\beta = 1/8$ at the quantum phase transition $|\lambda| = 1$ [see Figs. 2(a) and 2(c)]. Contrary to this, the dielectric polarization is governed by the formula

$$p \equiv \langle p_i^y \rangle = \frac{1}{2\pi} \frac{E}{\sqrt{J_H^2 + E^2}} [(1 + |\lambda|)\mathbf{E}(a) + (1 - |\lambda|)\mathbf{K}(a)], \quad (8)$$

where $\mathbf{K}(a) = \int_0^{\pi/2} d\phi (1 - a^2 \sin^2 \phi)^{-1/2}$ is the complete elliptic integral of the first kind. Formula (8) implies a smoother change of the dielectric polarization with only a weak-type singularity $|p - p_c| \sim (E - E_c) \ln |E - E_c|$ when crossing the respective ground-state phase boundary [see Figs. 2(b) and 2(c)]. Note furthermore that the dielectric polarization is much higher in the disordered QPM phase than in the ordered Néel and SL phases as evidenced by a density plot displayed in Fig. 2(b). The weak singularity of p at the quantum critical point [a solid circle in Fig. 2(c)] is more markedly evidenced through a logarithmic divergence of the dielectric susceptibility $\chi_d = \frac{\partial p}{\partial E} \sim -\ln |E - E_c|$ at the critical electric field E_c , as shown in Fig. 2(d).

IV. MEE IN NONZERO MAGNETIC FIELD

Two other ground states may emerge due to a nonzero magnetic field ($h \neq 0$). At high enough magnetic fields one may detect the classical ferromagnetic (FM) phase

characterized by

$$\mathcal{E}_{\text{FM}} = \frac{J_H}{4} + \frac{J_I}{2} - h, \quad m_s^z = 0, \quad p = 0, \quad \chi_d = 0. \quad (9)$$

In addition, the staggered bond (SB) phase with a regular alternation of singlet and polarized triplet states characterized by

$$\mathcal{E}_{\text{SB}} = -\frac{1}{4}\sqrt{J_H^2 + E^2} - \frac{h}{2}, \quad m_s^z = \frac{1}{4},$$

$$p = \frac{1}{4} \frac{E}{\sqrt{J_H^2 + E^2}}, \quad \chi_d = \frac{1}{4} \frac{J_H^2}{(J_H^2 + E^2)^{3/2}}, \quad (10)$$

may appear at moderate magnetic fields provided that the Ising intraleg coupling is of an antiferromagnetic nature $J_I > 0$. The typical ground-state phase diagram of the spin-1/2 Heisenberg-Ising ladder with ferromagnetic Ising intraleg coupling is illustrated in Fig. 3 in the form of density plots of the staggered magnetization m_s^z [Fig. 3(a)] and the dielectric polarization p [Fig. 3(b)] in the E/J_H - h/J_H plane. Obviously, Figs. 3(a) and 3(b) repeatedly imply a competitive character of the magnetic and dielectric spin orders when an enhancement of the dielectric polarization is accompanied with a reduction of the staggered magnetization or vice versa.

Furthermore, Figs. 3(c) and 3(d) display a few typical variations of the dielectric polarization and susceptibility across continuous and discontinuous phase transitions, which may

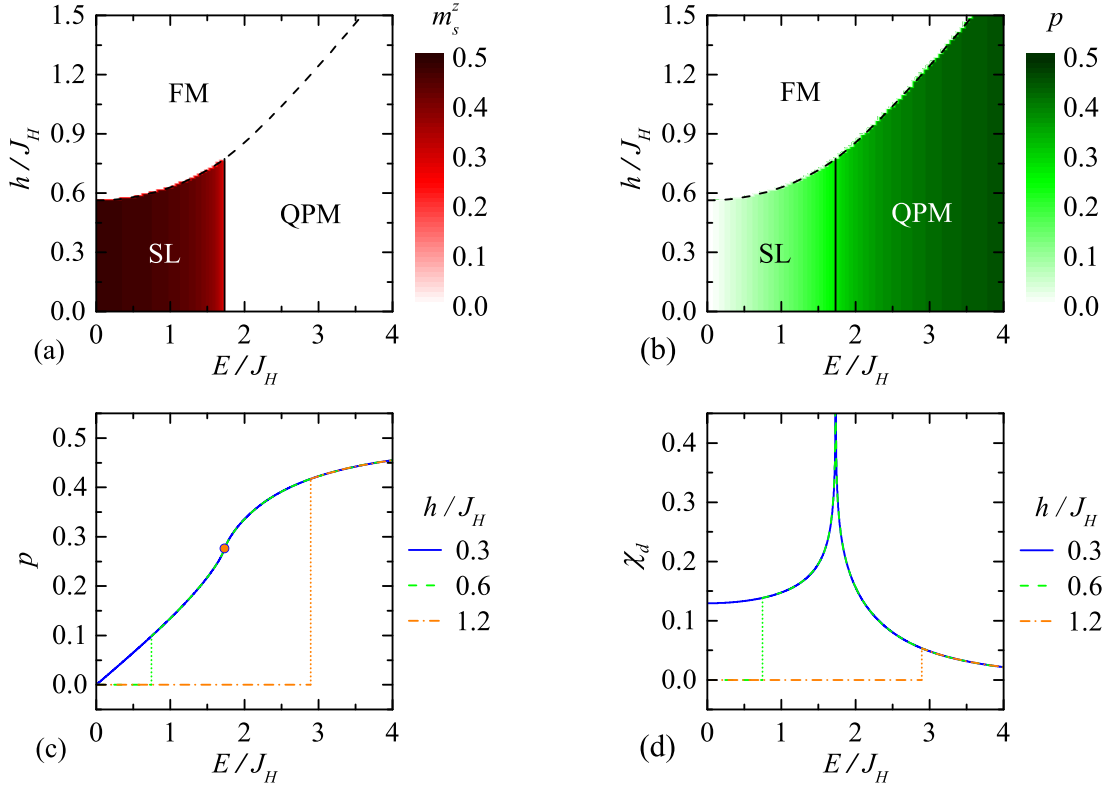


FIG. 3. The density plots of (a) the staggered magnetization m_s^z and (b) the dielectric polarization p as ground-state phase diagrams in the E/J_H - h/J_H plane for the interaction ratio $J_I/J_H = -2$ along with the electric field variations of (c) the dielectric polarization p and (d) the susceptibility χ_d for the interaction ratio $J_I/J_H = -2$ and three different magnetic fields $h/J_H = 0.3, 0.6, 1.2$.

be apparently controlled by external electric and magnetic fields. For sufficiently low magnetic fields (e.g., $h/J_H = 0.3$) the dielectric polarization displays a continuous rise with a weak singularity at the quantum phase transition between the SL and QPM phases [a solid circle in Fig. 3(c)], at which the dielectric susceptibility diverges logarithmically, as shown in Fig. 3(d). Contrary to this, the dielectric polarization and susceptibility may exhibit abrupt jumps related to a discontinuous phase transition between the FM and SL phases at moderate magnetic fields (e.g., $h/J_H = 0.6$) before achieving the electric-field-driven quantum phase transition SL-QPM.

As a comparison, a typical ground-state phase diagram of the spin-1/2 Heisenberg-Ising ladder with antiferromagnetic Ising intraleg coupling is displayed in Fig. 4 in the form of density plots of the staggered magnetization m_s^z [Fig. 4(a)] and the dielectric polarization p [Fig. 4(b)] in the E/J_H - h/J_H plane. Evidently, the main qualitative difference with respect to the previous case lies in the presence of a SB phase at moderate magnetic fields. Owing to this fact, one may detect a much greater versatility of the electric field variations of the dielectric polarization and susceptibility, as demonstrated in Figs. 4(c) and 4(d). At low enough magnetic fields (e.g., $h/J_H = 1.0$), the dielectric polarization exhibits a smooth continuous rise upon strengthening the electric field with a weak singularity at the respective quantum critical point [a solid circle in Fig. 4(c)], which becomes more evident

through a logarithmic divergence of the dielectric susceptibility [see Fig. 4(d)]. By contrast, one may detect a remarkable dependence of the dielectric polarization on the electric field with either one or two discontinuous jumps, which relate to discontinuous phase transitions driven by the external electric field at moderate and high magnetic fields (e.g., $h/J_H = 2.1, 2.5$, and 3.1).

V. CONCLUSIONS

To conclude, in the present paper, we have exactly examined a ground state of the spin-1/2 Heisenberg-Ising ladder in external electric and magnetic fields. It has been demonstrated that the ground-state spin arrangements may be basically manipulated through the MEE conditioned by the KNB mechanism via an external electric field, which additionally affords an alternative tool to control the quantum phase transition between the Néel (or stripy) quantum ordered phase and disordered quantum paramagnetic phase at zero magnetic field. It turns out, moreover, that an interplay between the electric and magnetic fields may cause the existence of either one or two discontinuous phase transitions as well as a single continuous quantum phase transition. Although the investigated quantum spin chain does not exhibit spontaneous multiferroic behavior, the feedback control of magnetic spin orderings through an external electric field might be of immense technological relevance because of the wide application potential of multifunctional materials.

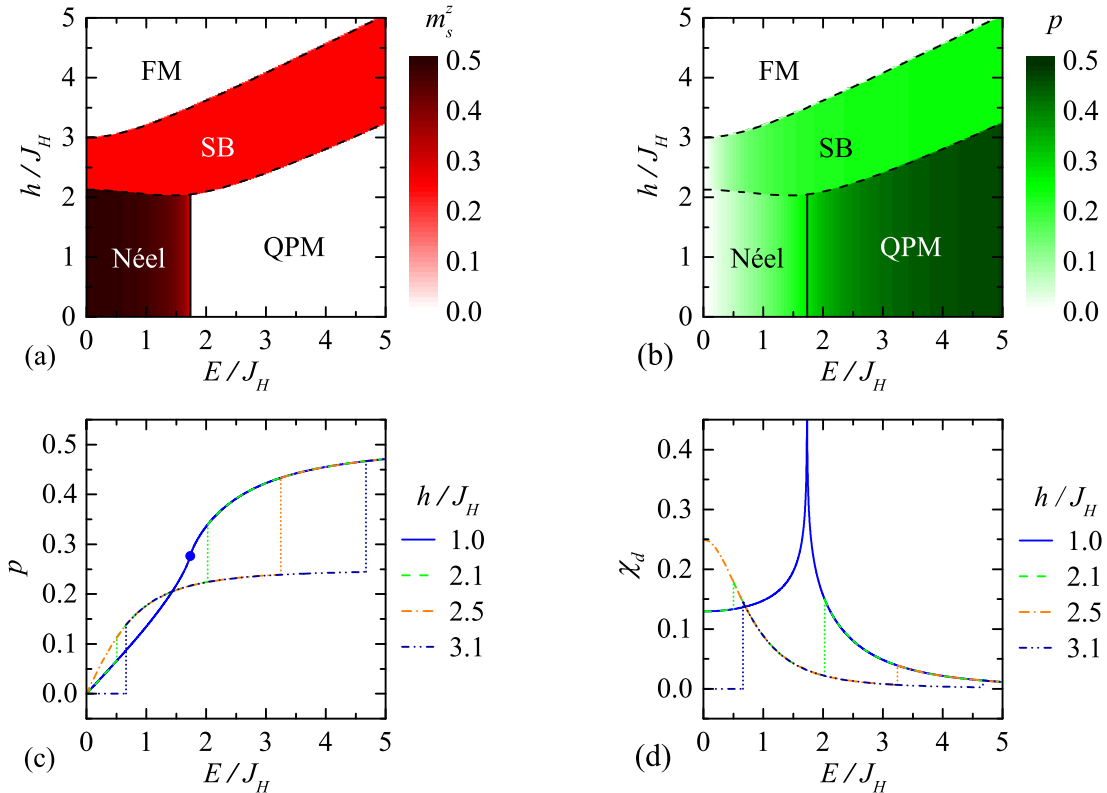


FIG. 4. The density plots of (a) the staggered magnetization m_s^z and (b) the dielectric polarization p as ground-state phase diagrams in the E/J_H - h/J_H plane for the interaction ratio $J_I/J_H = 2$ along with electric field variations of (c) the dielectric polarization p and (d) the susceptibility χ_d for the interaction ratio $J_I/J_H = 2$ and four different magnetic fields $h/J_H = 1.0, 2.1, 2.5, 3.1$.

ACKNOWLEDGMENTS

This work was supported by the Ministry of Education, Science, Research and Sport of the Slovak Republic under Grant No. VEGA 1/0043/16 and by the Slovak Research and Development Agency under Contract No. APVV-16-0186.

-
- [1] M. Fiebig, *J. Phys. D* **38**, R123 (2005), and references therein.
 [2] Y. Wang, J. Li, and D. Viehland, *Mater. Today* **17**, 269 (2014).
 [3] H. Katsura, N. Nagaosa, and A. V. Balatsky, *Phys. Rev. Lett.* **95**, 057205 (2005).
 [4] I. Dzyaloshinskii, *J. Phys. Chem. Solids* **4**, 241 (1958).
 [5] T. Moriya, *Phys. Rev.* **120**, 91 (1960).
 [6] Y. Yasui, Y. Naito, K. Sato, T. Moyoshi, M. Sato, and K. Kakurai, *J. Phys. Soc. Jpn.* **77**, 023712 (2008).
 [7] S. Seki, T. Kurumaji, S. Ishiwata, H. Matsui, H. Murakawa, Y. Tokunaga, Y. Kaneko, T. Hasegawa, and Y. Tokura, *Phys. Rev. B* **82**, 064424 (2010).
 [8] M. Brockmann, A. Klümper, and V. Ohanyan, *Phys. Rev. B* **87**, 054407 (2013).
 [9] O. Menchyshyn, V. Ohanyan, T. Verkholyak, T. Krokhumalskii, and O. Derzhko, *Phys. Rev. B* **92**, 184427 (2015).
 [10] J. Sznajd, *Phys. Rev. B* **97**, 214410 (2018).
 [11] O. Baran, V. Ohanyan, and T. Verkholyak, *Phys. Rev. B* **98**, 064415 (2018).
 [12] W.-L. You, G.-H. Liu, P. Horsch, and A. M. Oleś, *Phys. Rev. B* **90**, 094413 (2014).
 [13] I. Affleck and M. Oshikawa, *Phys. Rev. B* **60**, 1038 (1999).
 [14] T. Verkholyak and J. Strečka, *J. Phys. A: Math. Theor.* **45**, 305001 (2012).
 [15] T. Verkholyak and J. Strečka, *Condens. Matter Phys.* **16**, 13601 (2013).
 [16] W. Brzezicki and A. M. Oleś, *Eur. Phys. J. B* **66**, 361 (2008).
 [17] P. Pfeuty, *Ann. Phys. (NY)* **57**, 79 (1970).
 [18] R. J. Baxter, *Exactly Solved Models in Statistical Mechanics* (Academic Press, New York, 1982), pp. 32–38.